Published in final edited form as:
J Hypertens. 2011 November ; 29(11): 2116–2125. doi:10.1097/HJH.0b013e32834b22a0.

Genetic IL-10 Deficiency Causes Vascular Remodeling *via* the Upregulation of Nox1

Jagadeesha K. Dammanahalli, **Xiuqing Wang**, and **Zhongjie Sun**
Department of Physiology, College of Medicine, University of Oklahoma Health Sciences Center, Oklahoma City, Oklahoma, USA

Abstract

Background & Hypothesis—IL-10 is an anti-inflammatory cytokine. Nox1 is a mitogenic oxidase (p65-mox). The objective of this study was to test a hypothesis that IL10 deficiency would cause vascular remodeling *via* the upregulation of Nox1.

Methods & Results—Recombinant AAV carrying short hairpin small interference RNA for Nox1 (AAV.Nox1shRNA) was constructed for *in vivo* specific inhibition of Nox1. Three groups of IL10 gene knockout (IL10KO) mice and 3 groups of wild-type (WT) mice were used. Three groups of each strain received intravenous delivery of AAV.Nox1shRNA, AAV.ScrambledshRNA, and PBS, respectively. Animals were euthanized at 3 weeks after gene delivery. IL10KO increased Nox1 protein expression, NADPH oxidase activity, and superoxide production in aortas. IL10KO also resulted in a significant decrease in aortic medial thickness, a loss of smooth muscle cells, and an increase in vascular collagen deposition, indicating vascular remodeling. The IL10KO-induced increases in NADPH oxidase activity and superoxide production and vascular remodeling were abolished by silencing of p65-mox, suggesting that these effects may be mediated by the upregulation of Nox1. In addition, IL10KO increased endothelin-1 (ET-1) levels in plasma and aortas, and this effect was partially blocked by silencing of Nox1. RNAi silencing of Nox1 obliterated the IL10KO-induced increases in IL-6 expression in aortas, superoxide production and MMP-9 activity in aortic smooth muscle cells (SMC), and SMC migration.

Conclusions—IL10 is essential to the maintenance of normal vasculature as IL10 deficiency resulted in vascular damage and remodeling. The IL10KO-induced vascular structure damage may be mediated by the up-regulation of Nox1.

Keywords

vascular remodeling; vascular smooth muscle cell; AAV; IL-6; MMP-9; ET-1; NADPH oxidase; superoxide

Introduction

The vascular inflammatory status is determined by the balance of inflammatory and anti-inflammatory cytokines. Interleukin-10 (IL-10) is a pleiotropic cytokine that inhibits a broad

Address Correspondence to: Zhongjie Sun, MD, PhD, FAHA, Professor of Physiology, Department of Physiology, BMSB 662A, BOX 26901, College of Medicine, University of Oklahoma Health Sciences Center, 940 Stanton L. Young Blvd., Oklahoma City, OK 73104, USA., Tel. 405-271-2226 x 56237, Fax. 405-271-3181, zhongjie-sun@ouhsc.edu.

Conflict of Interest
Jagadeesha K. Dammanahalli: None declared
Xiuqing Wang: None declared
Zhongjie Sun: None declared

array of immune parameters with well known anti-inflammatory and immunosuppressive properties. IL-10 inhibits the production of cytokines such as IL-2, IL-6, and IL-8[1]. IL-10 downregulates the expression of ICAM-1 and VCAM-1 in IL-1–activated human umbilical vein endothelial cells (HUVECs) and decreases both IL-8 and IL-6 production in HUVECs[2]. IL-10 preserves the vascular function by inhibiting the production of proinflammatory cytokines and reactive oxygen species in endothelial cells[1, 3-4].

The NADPH oxidase is the major source of superoxide in the vascular wall[5-6]**.** Over the last decade, six homologues of gp91*phox* have been identified and named Nox 1-5[7-8]. Nox1 is an isoenzyme of gp91phox, termed mitogenic oxidase (p65-Mox)[8-10]. Recent studies indicated that Nox1 is expressed in vascular smooth muscle cells[11] and that overexpression of Nox1 promotes angiotensin II-induced hypertension[12]. Overexpression of Nox1 in NIH3T3 fibroblasts increases superoxide production and cell apoptosis and transformation[9]. Transfection of aortic smooth-muscle cells with Nox1 antisense decreased superoxide production[11].

It was reported that overexpression of IL-10 attenuates atherosclerosis, vascular dysfunction, and end organ damage[13-15]. IL10 deficiency increased ROS production leading to endothelial dysfunction[4]. It is not known, however, if IL-10 is involved in maintenance of normal vascular structure. The isoform of NADPH oxidases that mediates the IL10KO-induced increase in ROS production has never been determined. We hypothesize that IL-10 deficiency would cause vascular damage and remodeling *via* the upregulation of Nox1 NADPH oxidase activity. The aim of this study was to test this hypothesis by assessing the effect of RNAi silencing of Nox1 on vasculature in the IL10 gene knockout (IL10KO) mice.

Methods

For a full description of the Materials and Methods, please see the online Data Supplement.

Construction of recombinant adeno-associated virus (AAV-2) with Nox1-shRNA

Nox1-shRNA was designed using DHARMACON's software and synthesized by IDT DNA (Coralville, IA, USA). These sequences were designed to target on mouse Nox1 (p65-mox) at 5′-GATGCCTGGAAACTACCTA position in gene sequence: nucleotide 842–860. Nox1-shRNA was driven by human RNA polymerase III U6 promoter. The U6-Nox1shRNA was then packaged with pHelper and pAAV-RC to produce recombinant AAV.Nox1shRNA as described previously[16-19]. AAV with scrambled shRNA was also constructed to serve as a control construct (AAV.SC-shRNA). The scrambled (SC) shRNA has been proved by the BD Clontech (Palo Alto, CA, USA) not to match with any known gene sequences.

Animals

Three groups of IL-10 knockout (IL10KO) mice and 3 groups of wild-type (WT) mice (C57BL/6) (18-24 g, 8 weeks) were obtained from the Jackson Laboratories (Bar Harbor, ME, USA). The complete deletion of IL10 gene in IL10KO mice was confirmed by genotyping. Mice were provided with a standard rodent chow and tap water. All mice were housed at room temperature for 12h dark and 12h light throughout the experiment. The studies were performed according to the Guide for the Care and Use of Laboratory animals published by the US National Institute of Health (NIH Publication No. 85-23, revised 1996). The animal use protocols were approved by the Institutional Animal Care and Use Committee (IACUC) of the University of Oklahoma Health Sciences Center (OUHSC). The OUHSC ethical policy conforms with that of the NIH.

Body weight (BW) was measured twice a week. Following the control period, the three groups of each strain received AAV.Nox1shRNA, AAV.SCshRNA, and phosphate buffer solution (PBS), respectively. The viral particles were delivered intravenously (IV) at 1.25×10^9 particles/mouse (0.1 ml).

Measurement of ET-1 in plasma and aorta

Three weeks after gene delivery, all mice were euthanized (sodium pentobarbital, 120 mg/kg, IP). Blood was collected in a heparinized syringe *via* a cardiac puncture. Plasma was separated after centrifugation for measurements of ET-1s. Briefly, plasma samples was diluted in 1:4 ratio with assay buffer (Assay Design), mixed with an equal volume of 20% acetic acid, and evaporated to dryness. The assay was carried out using an ET-1 assay kit according to manufacturer's instructions (Assay Design). The values were expressed pg/ml plasma.

The frozen aorta was pulverized in the presence of liquid nitrogen and suspended in 1 M acetic acid and 2 mM HCl at 25°C. The suspensions were placed in a 100°C water bath for 3 min and then homogenized. The homogenates were centrifuged for 30 min at 4°C. The supernatant was collected and evaporated to dryness using a centrifugal concentrator under vacuum. The samples were reconstituted in 250 μl assay buffer and used for measuring ET-1 concentration using an ELISA kit (Assay Design) according to the manufacturer's instruction.

Morphological analysis and in situ superoxide production

Following perfusion, a part of the ascending aorta was postfixed overnight in 4% paraformaldehyde and then processed for paraffin embedding for morphological and histological analysis. Briefly, aortas was cut at 6-8 μm and mounted on slides. Tissue slices was stained with Hemotoxilin & Eosin (HE) for morphometric measurements. Aortic medial thickness and medial layer area were measured in ten consecutive aortic sections for each animal. Smooth muscle cells was confirmed with α-SMA antibody and counted using the imaging J software (SMCs/mm^2). Images were visualized and digital photographs were taken using a Nikon fluorescence microscope. The aortic collagen deposition was evaluated using Masson-Trichrome staining as we described recently[19-20]. The collagen staining was evaluated by examining ten randomly selected fields. Blue-stained areas were quantified using a color image analyzer. Collagen deposition was expressed as the percentage of the blue-stained area to the total aortic wall area (collagen area fraction).

A small segment of aorta was excised rapidly and processed for determination of *in situ* vascular superoxide production using DHE staining as described in our recent study[19-20].

Quantification of NAD(P)H oxidase activity

NADPH oxidase activity was assessed in the aortas using the lucigenin chemiluminescence method. To prevent autoxidation of lucigenin, a low concentration (5 μmol/l) of lucigenin was used, as previously described[21] with the following modifications. Tissue sections (40 u) were rinsed in ice-cold PBS and kept in 96-well plate in cold saline on ice for 10 min. Sections were incubated with lucigenin in the dark for 15 min. Background counts were then obtained by measuring chemiluminescence using a luminometer (Biotek synergy 2 Luminometer) for 5 min (with a 2-min dark adjustment). To evaluate NAD(P)H oxidase activity, 100 μM NAD(P)H was then added to samples, and luminescence was measured for an additional 8 min. Background counts (with lucigenin) were subtracted from each value. Lucigenin chemiluminescent counts were adjusted on the basis of protein concentration from tissue sections. Activity was expressed as relative light units (RLU)/per mg protein.

Western blot analysis

Western blot analysis was used for measuring Nox1, Nox2, Nox4, IL-4, IL-10 (Santa Cruz) and IL-6 (Abcam) in aortas. β-actin (Santa Cruz) was run as an internal control. Nox3 and Nox4 protein expression was undetectable in aortas. Nox5 is not expressed in the rodents[22]. For the detailed procedure, please see the online data supplement.

Isolation of vascular smooth muscle cell (VSMC)

Mouse aortic smooth muscle cells were isolated by enzymatic digestion as described earlier[23]. Briefly, aortas were incubated with digestion medium (Dulbecco's Modified Eagles Medium, DMEM, 0.5 mg/ml elastase, 1.0 mg/ml collagenase and 1.25 mg/ml trypsin) at 37 °C for 5 min. The adventitial layers of the blood vessels were then peeled off with forceps, and digestion medium was flushed through the vessel lumen to dislodge endothelial cells. The remaining tube of medial smooth muscle cells was then cut into segments (2–3 mm) and transferred to a micro centrifuge tube containing 500 μL of digestion medium. After incubating for 90 min at 37°C, VSMCs were dispersed with a P_{1000} pipette tip and plated onto a 60-mm culture dish containing 5 mL DMEM supplemented with 10% fetal bovine serum (FBS), 2 mmol/L L-glutamine, 100 U/mL penicillin, and 100 μg/mL streptomycin. The cells were maintained at 37 °C in a 5% CO_2 humidified incubator. Experiments were performed in VSMCs between passage 2-5 in the serum-deprived conditions (DMEM containing 0.1% FBS).

MMP-9 activity assay using gelatin zymography

Twenty-four hours before determining the levels of MMP-9, VSMCs were deprived of bovine serum to avoid background MMP activity from the serum. MMP-9 levels were determined in conditioned media, using gelatin zymography as described previously[24-25]. Briefly, 15 μL of conditioned media was mixed with 2x SDS buffer and the sample was incubated at room temperature for 10 min before loaded onto 10% gelatin Zymogram gels (Bio-Rad). After electrophoresis, gels were incubated with 1X renaturation buffer (Invitrogen) to remove SDS, and further incubated for 48h in developing buffer (Invitrogen) at 37°C. Gels were stained for 1 hr in coomassie blue (0.5% coomassie brilliant blue R-250, 30% methanol, 10% acetic acid) and destained in (30%:10%) methanol–acetic acid until proper contrast was achieved. The MMP-9 activity was detected as a white band on a dark blue background and quantified densitometrically.

VSMC migration

The migration of VSMCs was determined using a scratch wound assay as described previously[24]. Briefly, VSMCs were grown in 60-mm dishes until they reach confluence. The serum-starved VSMC monolayer was disrupted with a sterile cell scraper to create a cell-free zone. To quantify a leading front of cell migration, images were photographed at 0 h and 48 h later using a microscope equipped with a digital camera. The images were analyzed using an Olympus software IX-70. To ensure that images of the same area were taken at both time points, a straight horizontal line (perpendicular to the scratch wounds) was made on the underside of each well, and this was positioned at the bottom of each field before images were acquired.

Measurements of superoxide generation in VSMC

The superoxide generation in VSMCs was measured as described previously[26]. Briefly, the isolated VSMCs were harvested with trypsin, resuspended in colorless HBSS (10^6 cells/mL), and incubated in the dark for 30 min at 37°C in 5% CO_2 with 5 μmol/L dihydroethidium (DHE, Molecular probes). Flow cytometry (FACScan, Becton Dickinson) was used to select a homogeneous population of 10,000 live cells based on forward and side

scatter. The geometric mean of ethidium fluorescence intensity (excitation 488 nm, emission 585 nm) in the population was used for analysis. The red fluorescence channel was used to collect the DHE signal. The background fluorescence was determined in control cells without DHE staining. The background fluorescence was subtracted from the total readings. Mean fluorescence intensity was obtained from three separate experiments for each sample.

Statistical Analysis

Data were analyzed by two-way ANOVA followed by one-way ANOVA and Bonferroni multiple-comparisons between groups. Data are expressed as mean ± SEM. A p value <0.05 was considered statistical significance.

Results

Nox1shRNA reversed the IL10KO-induced increases in Nox1 expression and NADPH oxidase activity

Western blot analysis showed that Nox1 protein expression was increased significantly in aortas in IL10KO mice (Fig. 1A), suggesting that IL10KO upregulated Nox1 protein expression. The NADPH oxidase activity was measured based on superoxide generation by quantifying lucigenin chemiluminescence. IL10KO significantly increased NADPH oxidase activity in aortas (Fig. 1B). AAV delivery of Nox1shRNA abolished the upregulation of aortic Nox1 expression in IL10KO mice, indicating effective silencing of Nox1. The IL10KO-induced increase in NADPH oxidase activity was obliterated by Nox1shRNA (Fig. 1B), suggesting that the increase in NADPH oxidase activity may be due to the upregulation of Nox1 in the IL10KO mice. On the other hand, Nox2 protein expression levels were not altered in aortas (Online Data Supplement, S2).

IL10KO or AAV delivery of Nox1shRNA did not affect body weight significantly (Online Data Supplement, S1).

Nox1shRNA attenuated the in situ aortic superoxide production in IL10KO mice

The *in situ* vascular superoxide production was assessed using the DHE staining. The aortic superoxide production was increased significantly in IL10KO mice compared with the WT mice (Fig. 2A&B), indicating that IL10KO increased superoxide production. AAV delivery of Nox1shRAN reversed the IL10KO-induced increase in superoxide production (Fig. 2A&B), suggesting that the increase in superoxide production was due to the upregulation of Nox1.

Nox1shRNA decreased IL-6 expression and ET-1 production in IL10KO mice

IL-6 protein expression was increased significantly in aorta in the IL10KO mice compared with the WT mice (Fig. 3A), indicating that IL10KO upregulated IL-6 expression. Gene delivery of Nox1shRNA abolished the IL10KO-induced upregulation of IL-6 (Fig. 3A), suggesting that the upregulation of IL-6 may be mediated by the increase in Nox1 and superoxide production.

To determine whether IL-10 deficiency affects the ET-production, we measured ET-1 levels in plasma and aorta. The ET-1 levels in plasma (Fig. 3B) and aorta (Fig. 3C) were increased significantly in the IL10KO mice compared with the WT mice, indicating that IL10KO increased ET-1 production. Gene delivery of Nox1shRNA significantly decreased but did not prevent the IL10KO-induced increase in ET-1 levels (Fig. 3B,C), suggesting that the increase in ET-1 production may be partially mediated by the upregulation of Nox1.

Nox1shRNA decreased cell migration, superoxide production, and MMP-9 activity in VSMCs in IL10KO mice

The VSMC migration was assessed by the wound scratch method. The number of traveling VSMCs (Fig. 4A,B,C) and the distance of VSMC migration (Fig. 4A,B,D) were increased significantly in the IL10KO mice compared with the WT mice, indicating that IL10KO increased VSMC migration. In contrast, gene delivery Nox1shRNA abolished VSMC migration (Fig. 4A-D), suggesting that the IL10KO-induced VSMC migration may be mediated by the upregulation of Nox1 expression and superoxide production. Indeed, superoxide production was increased by nearly 2.5 fold in VSMCs of IL10KO mice compared with that of the WT mice. RNAi silencing of Nox1 abolished the IL10KO-induced superoxide production in VSMCs of IL10KO mice (Fig. 4E). Nox1 was still effectively silenced by AAV.Nox1shRNA in cultured SMCs for up to 5 passages).

Extracellular matrix (ECM) turnover is regulated by matrix metalloproteinases (MMPs). MMP-9 is an important MMP that degrades vascular elastin fibers, which promotes collagen deposition and smooth muscle cell migration. Basal activity of MMP-9 was increased significantly in the IL10KO group compared with the WT group (Fig. 4F), indicating the upregulation of MMP-9 activity. Gene transfer of Nox1shRNA reversed the upregulated MMP-9 activity in the IL10KO group, suggesting an important role of Nox1 in mediating the IL10KO-induced upregulation of MMP-9 activity (Fig. 4F).

Nox1shRNA decreased aortic collagen deposition in IL10KO mice

IL10KO significantly increased collagen deposition (blue) in aortas (Fig. 5A&B), a sign of fibrosis and vascular damage. Heavy collagen staining was found in both the SMC layer and the adventitial layer (Fig. 5A). Gene delivery of Nox1shRNA abolished the IL10KO-induced collagen deposition in aortas (Fig. 5A&B), suggesting that the fibrotic formation may be mediated by the upregulation of Nox1 expression and superoxide production.

Nox1shRNA attenuated vascular damage in IL10KO mice

The medial thickness was decreased significantly in aortas of IL10KO mice (Fig. 8A-C). There was a loss of SMCs in aortas in IL10KO mice (Fig. 6A-D). These results indicated vascular structure damage. The IL10KO-induced vascular damage may be due to the upregulation of Nox1 expression because it can be abolished by RNAi silencing of Nox1 (Fig. 6A-D).

Discussion

This study demonstrated that IL10 gene knockout caused vascular structure damage and remodeling as evidenced by a loss of VSMCs, an increase in vascular collagen deposition, and vascular atrophy. This finding reveals, for the first time, that the anti-inflammatory cytokine IL10 is essential to the maintenance of normal vascular structure. The inflammatory status is balanced by inflammatory cytokines (e.g., IL6) and anti-inflammatory cytokines (e.g., IL10). A decrease in anti-inflammatory cytokines and/or an increase in inflammatory cytokines would cause an inflammatory status. Because IL-10 can attenuate expression and/or production of inflammatory cytokines[4, 27], it is not surprising that IL10 deficiency resulted in an upregulation of IL6 expression in aortas although the cell source of IL6 remains to be determined. Cytokines and inflammation may be involved in the pathogenesis of vascular dysfunction, hypertension and organ damage[28-29]. IL-10 likely exerts its anti-inflammatory effects on the vascular system through the inhibition of inflammatory cytokines such as IL-6. Several studies suggest that the *in vivo* expression of IL10 may inhibit the formation of atherosclerosis[13, 30] and ameliorate hypertension-related

end organ damages[14-15]. Therefore, IL-10 may be a natural endogenous defender for the cardiovascular system.

The IL10KO-induced vascular damage and remodeling may be due to upregulation of NADPH oxidase activity and superoxide production as it can be abolished by inhibition of NADPH oxidase by Nox1shRNA. NADPH oxidases are the major source of superoxide in the vascular system[6, 31-33]. It is well established that an increase in superoxide or ROS production is involved in vascular dysfunction, hypertension, and end organ damages[32, 34-36]. This study further revealed that the IL10KO-induced increase in NADPH oxidase activity is likely due to the upregulation of Nox1 as it could be abolished by RNAi silencing of Nox1. It is interesting that IL10KO upregulated a specific isoform of NADPH oxidases although the underlying mechanism remains to be determined. It seems that Nox1 is highly responsive to IL10KO. In contrast, Nox2 and Nox4 expression was not affected by IL10KO. Indeed, Nox1 is the primary NADPH oxidase that mediates the innate immune response in the gastrointestinal tract[37-38]. Several lines of evidence suggest that Nox1 may play a crucial role in the initiation of local innate immune response and inflammation[7, 37-39]. This is, to our knowledge, the first report showing that IL10 deficiency selectively upregulated vascular Nox1 expression. Whether there exists direct and specific relationship between IL10 and Nox1 is certainly an interesting topic to pursue. This finding further pointed out that the deleterious effects of IL10KO on blood vessels may be attributed to the upregulation of Nox1 because it could be reversed by specific silencing of Nox1.

It is noted that IL10KO resulted in an increase in ET-1 production. An increase in ET-1 production may cause vascular dysfunction and damage[31, 40-42]. The IL10KO-induced increase in ET-1 production may be partially mediated by the upregulation of Nox1 because it was attenuated by RNAi silencing of Nox1. Superoxide or ROS stimulates ET-1 release[31]. It was reported that IL10KO enhanced ETA-mediated vascular responses to ET-1 due to the upregulation of ETA receptors[43]. Therefore, the increase in ET-1 production and the enhanced vascular responses to ET-1 may contribute to vascular damage and remodeling in IL10KO mice.

Extracellular matrix (ECM) turnover is regulated by matrix metalloproteinases (MMPs). Numerous reports indicate that MMPs play an important role in the pathogenesis of vascular diseases such as arterial stiffening[44-45]. MMP-9 degrades vascular elastins, which promotes collagen deposition, leading to vascular remodeling and arterial stiffening[45-47]. It has been previously reported that production of MMP-9 is stimulated by several cytokines, such as IL-6 and TNF-α[48]. The present finding reveals that IL10KO upregulated MMP-9 activity, suggesting that IL-10 may be an important regulator of MMP9 activity. The IL10KO-induced activation of MMP-9 activity may be responsible for matrix degradation, loss of elastin fibers, and collagen deposition and thus vascular atrophy. The upregulation of Nox1 may mediate the IL10KO-induced increase in MMP-9 activity because it can be abolished by RNAi silencing of Nox1.

It is noted that there was a loss of SMCs in the IL10KO mice, which is likely due to the increased ROS production. Using flowcytometry, we found that the ROS production was upregulated in the isolated SMCs from the IL10KO mice. ROS could cause oxidative stress and apoptosis in SMCs[49-51]. Nox1 seems to be the major source of IL10KO-induced superoxide production in SMCs because it can be abolished by p65shRNA. The Nox1-derived ROS may also be responsible for the IL10KO-induced SMC migration which contributes to vascular remodeling. MMP-9 facilitates SMC migration *via* degrading extracellular matrix. It has been reported that Nox1 is the primary NADPH oxidase that is responsible for cell transformation and apoptosis[9, 52].

In summary, genetic IL10 deficiency resulted in vascular damage and remodeling, supporting a critical role of IL10 in the maintenance of normal vasculature. IL10KO upregulated expression of vascular Nox1 expression, which may mediate the IL10KO-induced vascular damage and remodeling.

Supplementary Material

Refer to Web version on PubMed Central for supplementary material.

Acknowledgments

This work was supported by the National Institute of Health (R01 HL105302).

References

1. Moore KW, de Waal Malefyt R, Coffman RL, O'Garra A. Interleukin-10 and the interleukin-10 receptor. Annu. Rev. Immunol. 2001; 19:683–765. [PubMed: 11244051]
2. Krakauer T. IL-10 inhibits the adhesion of leukocytic cells to IL-1-activated human endothelial cells. Immunol. Lett. 1995; 45(1-2):61–65. [PubMed: 7542627]
3. Barillari G, Albonici L, Incerpi S, Bogetto L, Pistritto G, Volpi A, Ensoli B, Manzari V. Inflammatory cytokines stimulate vascular smooth muscle cells locomotion and growth by enhancing alpha5beta1 integrin expression and function. Atherosclerosis. 2001; 154(2):377–385. [PubMed: 11166770]
4. Gunnett CA, Heistad DD, Berg DJ, Faraci FM. IL-10 deficiency increases superoxide and endothelial dysfunction during inflammation. Am J Physiol Heart Circ Physiol. 2000; 279(4):H1555–1562. [PubMed: 11009441]
5. Zemse SM, Hilgers RH, Webb RC. Interleukin-10 counteracts impaired endothelium-dependent relaxation induced by ANG II in murine aortic rings. Am J Physiol Heart Circ Physiol. 2007; 292(6):H3103–3108. [PubMed: 17322422]
6. Keaney JF Jr. Oxidative stress and the vascular wall: NADPH oxidases take center stage. Circulation. 2005; 112(17):2585–2588. [PubMed: 16246957]
7. Geiszt M, Leto TL. The Nox family of NAD(P)H oxidases: host defense and beyond. J. Biol. Chem. 2004; 279(50):51715–51718. [PubMed: 15364933]
8. Lambeth JD, Cheng G, Arnold RS, Edens WA. Novel homologs of gp91phox. Trends Biochem. Sci. 2000; 25(10):459–461. [PubMed: 11050424]
9. Suh YA, Arnold RS, Lassegue B, Shi J, Xu X, Sorescu D, Chung AB, Griendling KK, Lambeth JD. Cell transformation by the superoxide-generating oxidase Mox1. Nature. 1999; 401(6748):79–82. [PubMed: 10485709]
10. Banfi B, Maturana A, Jaconi S, Arnaudeau S, Laforge T, Sinha B, Ligeti E, Demaurex N, Krause KH. A mammalian H+ channel generated through alternative splicing of the NADPH oxidase homolog NOH-1. Science. 2000; 287(5450):138–142. [PubMed: 10615049]
11. Lassegue B, Sorescu D, Szocs K, Yin Q, Akers M, Zhang Y, Grant SL, Lambeth JD, Griendling KK. Novel gp91(phox) homologues in vascular smooth muscle cells: nox1 mediates angiotensin II-induced superoxide formation and redox-sensitive signaling pathways. Circ. Res. 2001; 88(9): 888–894. [PubMed: 11348997]
12. Dikalova A, Clempus R, Lassegue B, Cheng G, McCoy J, Dikalov S, San Martin A, Lyle A, Weber DS, Weiss D, Taylor WR, Schmidt HH, Owens GK, Lambeth JD, Griendling KK. Nox1 overexpression potentiates angiotensin II-induced hypertension and vascular smooth muscle hypertrophy in transgenic mice. Circulation. 2005; 112(17):2668–2676. [PubMed: 16230485]
13. Yoshioka T, Okada T, Maeda Y, Ikeda U, Shimpo M, Nomoto T, Takeuchi K, Nonaka-Sarukawa M, Ito T, Takahashi M, Matsushita T, Mizukami H, Hanazono Y, Kume A, Ookawara S, Kawano M, Ishibashi S, Shimada K, Ozawa K. Adeno-associated virus vector-mediated interleukin-10 gene transfer inhibits atherosclerosis in apolipoprotein E-deficient mice. Gene Ther. 2004; 11(24): 1772–1779. [PubMed: 15496963]

14. Nomoto T, Okada T, Shimazaki K, Yoshioka T, Nonaka-Sarukawa M, Ito T, Takeuchi K, Katsura KI, Mizukami H, Kume A, Ookawara S, Ikeda U, Katayama Y, Ozawa K. Systemic delivery of IL-10 by an AAV vector prevents vascular remodeling and end-organ damage in stroke-prone spontaneously hypertensive rat. Gene Ther. 2009; 16(3):383–391. [PubMed: 18818668]
15. Nonaka-Sarukawa M, Okada T, Ito T, Yamamoto K, Yoshioka T, Nomoto T, Hojo Y, Shimpo M, Urabe M, Mizukami H, Kume A, Ikeda U, Shimada K, Ozawa K. Adeno-associated virus vector-mediated systemic interleukin-10 expression ameliorates hypertensive organ damage in Dahl salt-sensitive rats. J Gene Med. 2008; 10(4):368–374. [PubMed: 18205252]
16. Sun Z, Bello-Roufai M, Wang X. RNAi inhibition of mineralocorticoid receptors prevents the development of cold-induced hypertension. Am J Physiol Heart Circ Physiol. 2008; 294(4):H1880–1887. [PubMed: 18296563]
17. Wang X, Skelley L, Cade R, Sun Z. AAV delivery of mineralocorticoid receptor shRNA prevents progression of cold-induced hypertension and attenuates renal damage. Gene Ther. 2006; 13(14): 1097–1103. [PubMed: 16554840]
18. Wang X, Sun Z. RNAi silencing of brain klotho potentiates cold-induced elevation of blood pressure via the endothelin pathway. Physiol Genomics. 2010
19. Wang Y, Sun Z. Klotho gene delivery prevents the progression of spontaneous hypertension and renal damage. Hypertension. 2009; 54(4):810–817. [PubMed: 19635988]
20. Zuo Z, Lei H, Wang X, Wang Y, Sonntag W, Sun Z. Aging-related kidney damage is associated with a decrease in klotho expression and an increase in superoxide production. Age (Dordr). 2010; 10:10.
21. Rey FE, Cifuentes ME, Kiarash A, Quinn MT, Pagano PJ. Novel competitive inhibitor of NAD(P)H oxidase assembly attenuates vascular O(2)(-) and systolic blood pressure in mice. Circ. Res. 2001; 89(5):408–414. [PubMed: 11532901]
22. Schulz E, Munzel T. NOX5, a new “radical” player in human atherosclerosis? J Am Coll Cardiol. 2008; 52(22):1810–1812. [PubMed: 19022161]
23. Ray JL, Leach R, Herbert JM, Benson M. Isolation of vascular smooth muscle cells from a single murine aorta. Methods Cell Sci. 2001; 23(4):185–188. [PubMed: 12486328]
24. Galis ZS, Johnson C, Godin D, Magid R, Shipley JM, Senior RM, Ivan E. Targeted disruption of the matrix metalloproteinase-9 gene impairs smooth muscle cell migration and geometrical arterial remodeling. Circ. Res. 2002; 91(9):852–859. [PubMed: 12411401]
25. Godin D, Ivan E, Johnson C, Magid R, Galis ZS. Remodeling of carotid artery is associated with increased expression of matrix metalloproteinases in mouse blood flow cessation model. Circulation. 2000; 102(23):2861–2866. [PubMed: 11104745]
26. Dammanahalli JK, Sun Z. Endothelin (ET)-1 inhibits nicotinamide adenine dinucleotide phosphate oxidase activity in human abdominal aortic endothelial cells: a novel function of ETB1 receptors. Endocrinology. 2008; 149(10):4979–4987. [PubMed: 18535108]
27. Parker JL, Myers PR, Zhong Q, Kim K, Adams HR. Inhibition of endothelium-dependent vasodilation by Escherichia coli endotoxemia. Shock. 1994; 2(6):451–458. [PubMed: 7538038]
28. Vila E, Salaices M. Cytokines and vascular reactivity in resistance arteries. Am J Physiol Heart Circ Physiol. 2005; 288(3):H1016–1021. [PubMed: 15706038]
29. Crosswhite P, Sun Z. Nitric oxide, oxidative stress and inflammation in pulmonary arterial hypertension. J. Hypertens. 2010; 28(2):201–212. [PubMed: 20051913]
30. Mallat Z, Besnard S, Duriez M, Deleuze V, Emmanuel F, Bureau MF, Soubrier F, Esposito B, Duez H, Fievet C, Staels B, Duverger N, Scherman D, Tedgui A. Protective role of interleukin-10 in atherosclerosis. Circ. Res. 1999; 85(8):e17–24. [PubMed: 10521249]
31. Dammanahalli KJ, Sun Z. Endothelins and NADPH oxidases in the cardiovascular system. Clin. Exp. Pharmacol. Physiol. 2008; 35(1):2–6. [PubMed: 18047620]
32. Cai H, Griendling KK, Harrison DG. The vascular NAD(P)H oxidases as therapeutic targets in cardiovascular diseases. Trends Pharmacol. Sci. 2003; 24(9):471–478. [PubMed: 12967772]
33. Griendling KK, Sorescu D, Ushio-Fukai M. NAD(P)H oxidase: role in cardiovascular biology and disease. Circ. Res. 2000; 86(5):494–501. [PubMed: 10720409]
34. Fortuno A, San Jose G, Moreno MU, Diez J, Zalba G. Oxidative stress and vascular remodelling. Exp. Physiol. 2005; 90(4):457–462. [PubMed: 15890797]

35. Wassmann S, Nickenig G. Interrelationship of free oxygen radicals and endothelial dysfunction--modulation by statins. Endothelium. 2003; 10(1):23–33. [PubMed: 12699074]
36. Rajagopalan S, Kurz S, Munzel T, Tarpey M, Freeman BA, Griendling KK, Harrison DG. Angiotensin II-mediated hypertension in the rat increases vascular superoxide production via membrane NADH/NADPH oxidase activation. Contribution to alterations of vasomotor tone. J. Clin. Invest. 1996; 97(8):1916–1923. [PubMed: 8621776]
37. Rokutan K, Kawahara T, Kuwano Y, Tominaga K, Nishida K, Teshima-Kondo S. Nox enzymes and oxidative stress in the immunopathology of the gastrointestinal tract. Semin Immunopathol. 2008; 30(3):315–327. [PubMed: 18521607]
38. Rokutan K, Kawahara T, Kuwano Y, Tominaga K, Sekiyama A, Teshima-Kondo S. NADPH oxidases in the gastrointestinal tract: a potential role of Nox1 in innate immune response and carcinogenesis. Antioxid Redox Signal. 2006; 8(9-10):1573–1582. [PubMed: 16987012]
39. Leto TL, Geiszt M. Role of Nox family NADPH oxidases in host defense. Antioxid Redox Signal. 2006; 8(9-10):1549–1561. [PubMed: 16987010]
40. Agapitov AV, Haynes WG. Role of endothelin in cardiovascular disease. J Renin Angiotensin Aldosterone Syst. 2002; 3(1):1–15. [PubMed: 11984741]
41. Ferro CJ, Haynes WG, Johnston NR, Lomax CC, Newby DE, Webb DJ. The peptide endothelin receptor antagonist, TAK-044, produces sustained inhibition of endothelin-1 mediated arteriolar vasoconstriction. Br. J. Clin. Pharmacol. 1997; 44(4):377–383. [PubMed: 9354313]
42. Touyz RM, Schiffrin EL. Role of endothelin in human hypertension. Can. J. Physiol. Pharmacol. 2003; 81(6):533–541. [PubMed: 12839265]
43. Giachini FR, Zemse SM, Carneiro FS, Lima VV, Carneiro ZN, Callera GE, Ergul A, Webb RC, Tostes RC. Interleukin-10 attenuates vascular responses to endothelin-1 via effects on ERK1/2-dependent pathway. Am J Physiol Heart Circ Physiol. 2009; 296(2):H489–496. [PubMed: 19074677]
44. Loftus IM, Thompson MM. The role of matrix metalloproteinases in vascular disease. Vasc. Med. 2002; 7(2):117–133. [PubMed: 12402992]
45. Bouvet C, Moreau S, Blanchette J, de Blois D, Moreau P. Sequential activation of matrix metalloproteinase 9 and transforming growth factor beta in arterial elastocalcinosis. Arterioscler. Thromb. Va~c. Biol. 2008; 28(5):856–862.
46. Medley TL, Cole TJ, Dart AM, Gatzka CD, Kingwell BA. Matrix metalloproteinase-9 genotype influences large artery stiffness through effects on aortic gene and protein expression. Arterioscler. Thromb. Va~c. Biol. 2004; 24(8):1479–1484.
47. Hindson VJ, Ashworth JL, Rock MJ, Cunliffe S, Shuttleworth CA, Kielty CM. Fibrillin degradation by matrix metalloproteinases: identification of amino- and carboxy-terminal cleavage sites. FEBS Lett. 1999; 452(3):195–198. [PubMed: 10386589]
48. Tazaki T, Minoguchi K, Yokoe T, Samson KT, Minoguchi H, Tanaka A, Watanabe Y, Adachi M. Increased levels and activity of matrix metalloproteinase-9 in obstructive sleep apnea syndrome. Am. J. Respir. Crit. Care Med. 2004; 170(12):1354–1359. [PubMed: 15361365]
49. Li WG, Miller FJ Jr. Brown MR, Chatterjee P, Aylsworth GR, Shao J, Spector AA, Oberley LW, Weintraub NL. Enhanced H(2)O(2)-induced cytotoxicity in “epithelioid” smooth muscle cells: implications for neointimal regression. Arterioscler. Thromb. Va~c. Biol. 2000; 20(6):1473–1479.
50. Pedruzzi E, Guichard C, Ollivier V, Driss F, Fay M, Prunet C, Marie JC, Pouzet C, Samadi M, Elbim C, O’Dowd Y, Bens M, Vandewalle A, Gougerot-Pocidalo MA, Lizard G, Ogier-Denis E. NAD(P)H oxidase Nox-4 mediates 7-ketocholesterol-induced endoplasmic reticulum stress and apoptosis in human aortic smooth muscle cells. Mol. Cell. Biol. 2004; 24(24):10703–10717. [PubMed: 15572675]
51. Jagadeesha DK, Lindley TE, Deleon J, Sharma RV, Miller F, Bhalla RC. Tempol therapy attenuates medial smooth muscle cell apoptosis and neointima formation after balloon catheter injury in carotid artery of diabetic rats. Am J Physiol Heart Circ Physiol. 2005; 289(3):H1047–1053. [PubMed: 15833798]
52. Arnold RS, Shi J, Murad E, Whalen AM, Sun CQ, Polavarapu R, Parthasarathy S, Petros JA, Lambeth JD. Hydrogen peroxide mediates the cell growth and transformation caused by the

mitogenic oxidase Nox1. Proc. Natl. Acad. Sci. U. S. A. 2001; 98(10):5550–5555. [PubMed: 11331784]

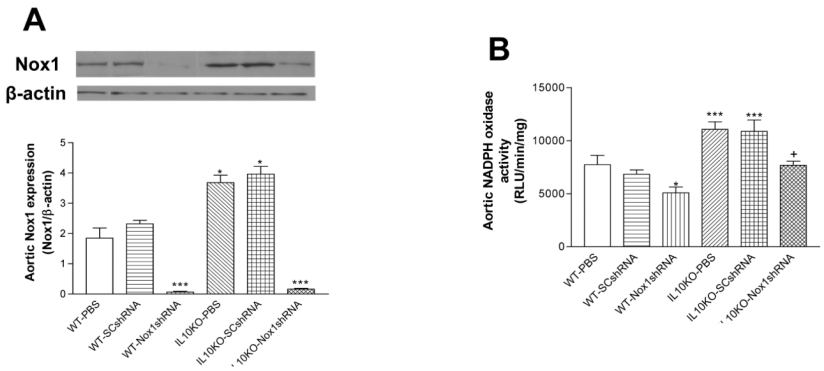

Figure 1. Effects of RNAi silencing of Nox1 on Nox1 expression and NADPH oxidase activity in aortas

Western blot analysis of Nox1 expression in aortas **(A)**. The NADPH oxidase activity in aortas **(B)**. Data=means±SE. *$p<0.05$, ***$p<0.001$ *vs* the WT-PBS group. $^{+}p<0.05$ *vs* the IL10KO-PBS group. N=5. PBS, phosphate buffer solution; SCshRNA, scrambled sequence of short hairpin siRNA; Nox1shRNA, shRNA for p65-mox (Nox1). N=5.

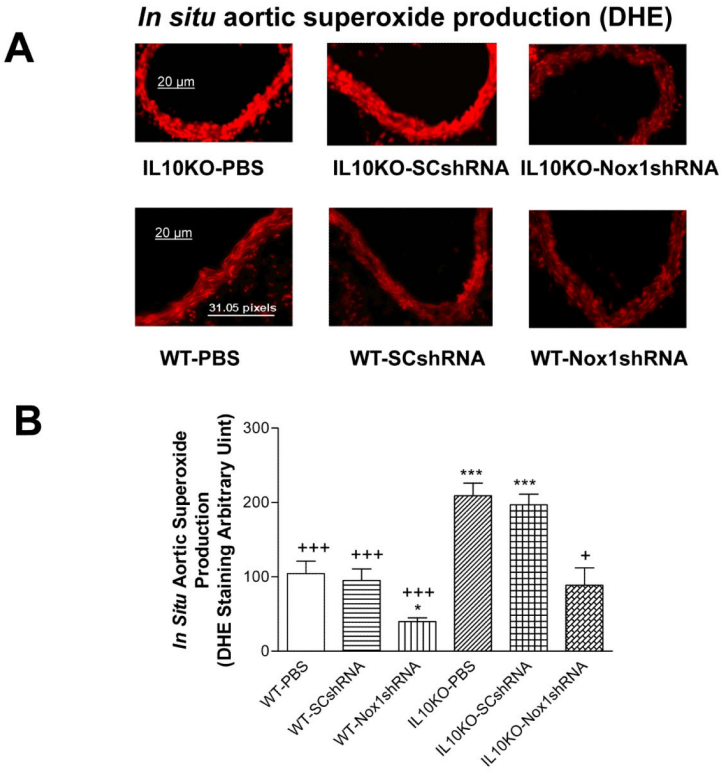

Figure 2. Effects of RNAi silencing Nox1 on *in situ* vascular superoxide production

Dihydroethidium (DHE) fluorescence in aortas **(A)**. Quantification of DHE fluorescence density **(B)**. Data=means±SE. *$p<0.05$, ***$p<0.001$ *vs* the WT-PBS group. $^{+}p<0.05$, $^{+++}p<0.001$ *vs* the IL10KO-PBS group. N=5.

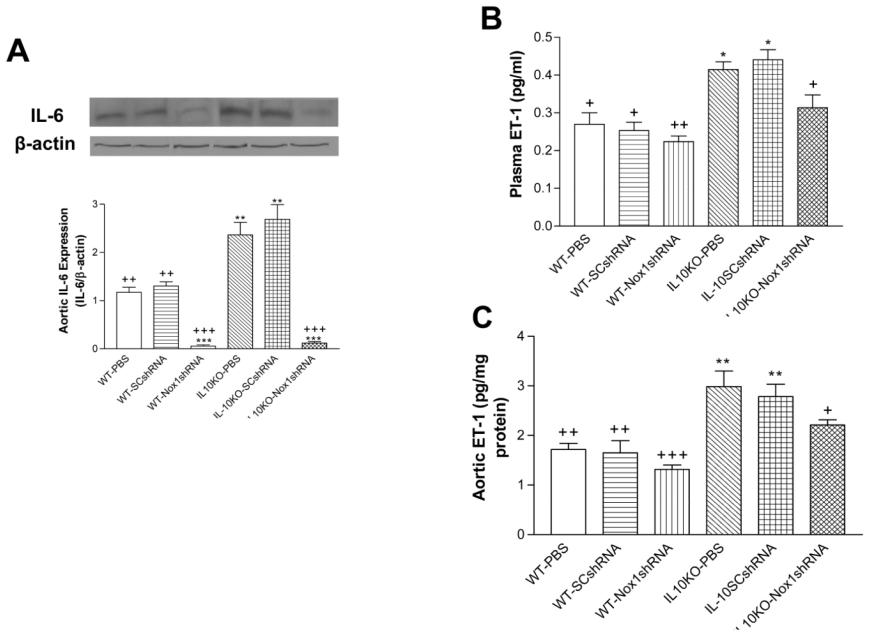

Figure 3. Effects of RNAi silencing of Nox1 on IL-6 expression and ET-1 production

IL-6 protein expression in aortas **(A)**. Plasma levels of ET-1 **(B)**. The aortic content of ET-1 **(C)**. Data=means±SE. *$p<0.05$, **$p<0.01$, ***$p<0.001$ *vs* the WT-PBS group. $^{+}p<0.05$,$^{++}p<0.01$ $^{+++}p<0.001$ *vs* the IL10KO-PBS group. N=5.

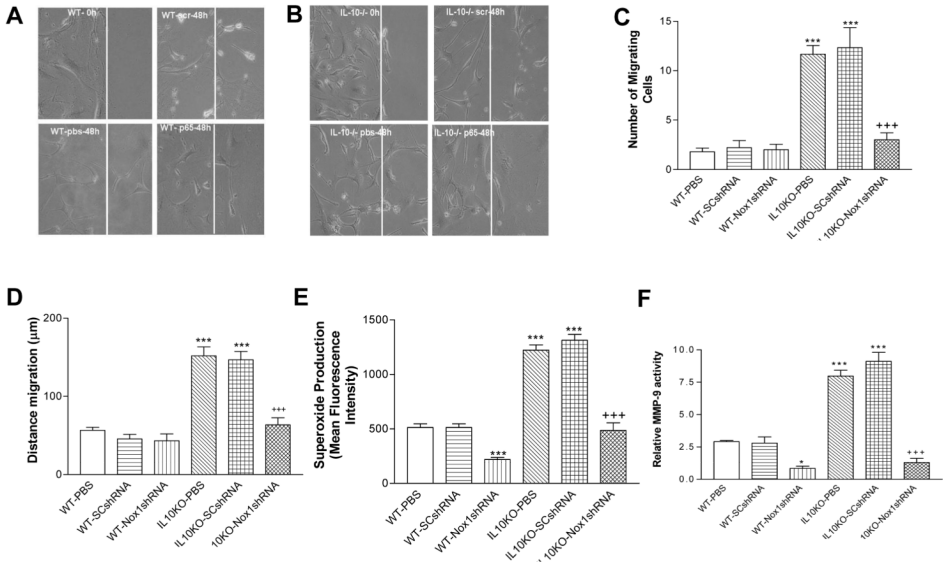

Figure 4. Effects of RNAi silencing of Nox1 on cell migration, ROS production and MMP-9 Activity in isolated and cultured smooth muscle cells (SMCs)

Confluent cells were allowed to grow for 48 h following wound injury. A photograph of cells migrated after 48 h in each group (**A&B**). Scr, scrambled shRNA. p65, Nox1shRNA. IL-10-/-, IL10 gene knockout. pbs, PBS (phosphate buffer solution). The summary data of the number of cells migrated and the average distance traveled (**C&D**). Aortic SMCs were exposed to the superoxide specific dye dihydroethidium (10 μM) for 30 min. Ethidium fluorescence was measured quantitatively by flow cytometry (**E**). MMP-9 activity was measured by gelatin zymography (**F**). Data=means±SE. *p<0.05, ***p<0.001 *vs* the WT-PBS group. ^{+++}p<0.001 *vs* the IL10KO-PBS group. N=5.

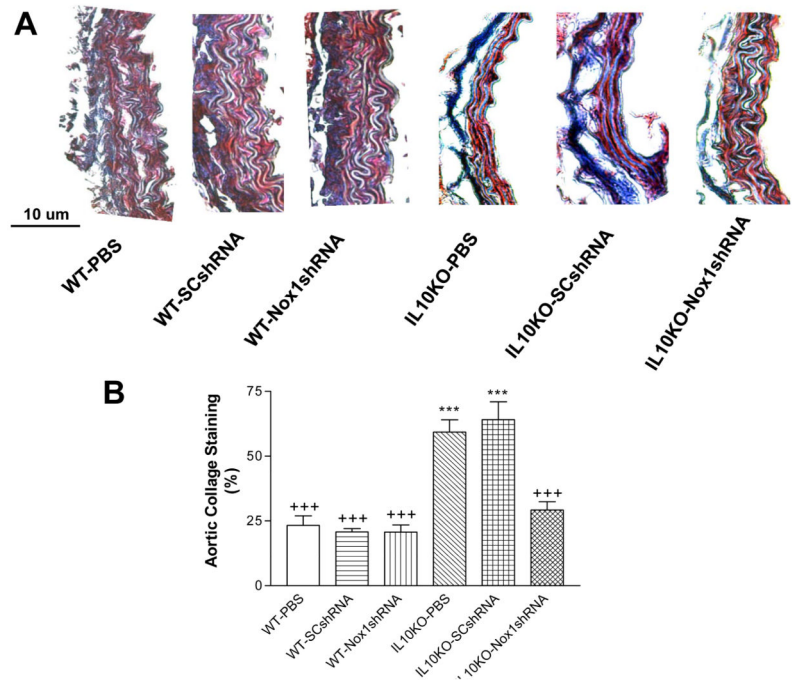

Figure 5. Effects of RNAi silencing of Nox1 on the aortic collagen content

Trichrome staining of the aorta sections (7 μM) from IL-10KO and WT mice. Heavy collagen staining (blue) was found in the SMC layer and the adventitial matrix in the IL10KO mice **(A)**. There was a loss of elastin fibers in the medial layer in the IL10KO mice **(A)**. Quantification of collagen content **(B).** Data=means±SE. ***$p<0.001$ *vs* the WT-PBS group. $^{+++}p<0.001$ *vs* the IL10KO-PBS group. N=5.

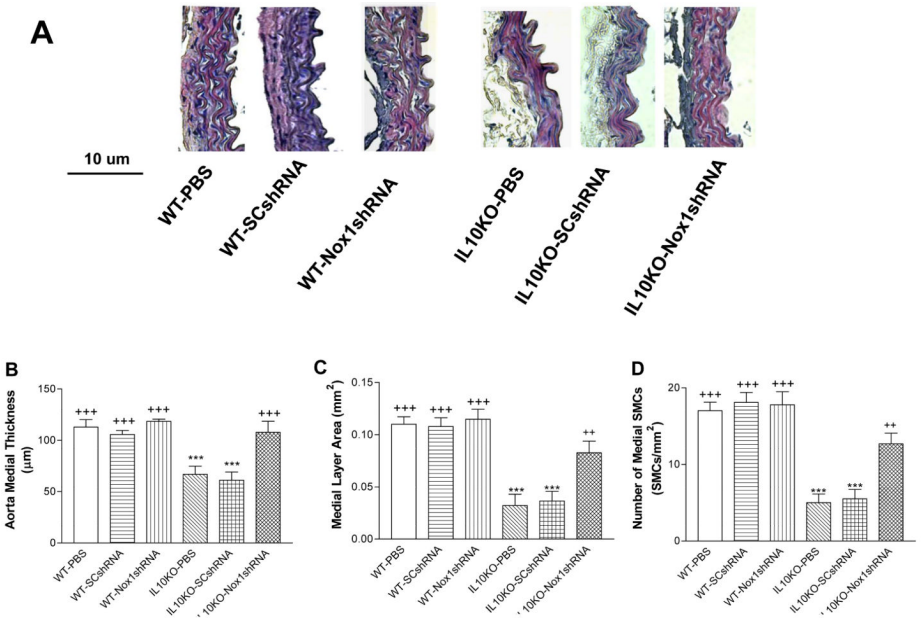

Figure 6. Effects of RNAi silencing of Nox1 on aortic medial layer remodeling

Hemotoxilin & Eosin (HE) staining of thoracic aortic sections (6 μM). Morphometric analysis of aortic medial layer of the IL10KO mice (**A**). Quantification of aortic medial thickness (**B**), aortic medial layer area **(C)**, and medial SMCs **(D)** after 21days of gene delivery. Data=means±SE. ***p<0.001 *vs* the WT-PBS group. ^{++}p<0.001, ^{+++}p<0.001 *vs* the IL10KO-PBS group. N=5.